Quench-induced breathing mode of one-dimensional Bose gases

Bess Fang, Giuseppe Carleo, Isabelle Bouchoule

Quench-induced breathing mode of one-dimensional Bose gases

Bess Fang, Giuseppe Carleo, and Isabelle Bouchoule
Laboratoire Charles Fabry, Institut d'Optique, Univ Paris Sud 11, 2 avenue Augustin Fresnel, F-91127 Palaiseau cedex, France
(Dated: December 10, 2013)

We measure the position- and momentum- space breathing dynamics of trapped one-dimensional Bose gases. The profile in real space reveals sinusoidal width oscillations whose frequency varies continuously through the quasicondensate to ideal Bose gas crossover. A comparison with theoretical models taking into account the effect of finite temperature is provided. In momentum space, we report the first observation of a frequency doubling in the quasicondensate regime, corresponding to a self-reflection mechanism. The disappearance of this mechanism through the quasicondensation crossover is mapped out.

PACS numbers: 03.75.Kk, 67.85.-d

The field of ultracold atomic and molecular gases has gained increasing significance in the study of nonequilibrium dynamics of quantum many-body systems. The high degree of control enables the realization of prototypical nonequilibrium processes, complementary to those studied in condensed matter physics. In particular, dynamics of isolated quantum many-body system can be addressed. The theoretical treatment of quantum dynamics in the presence of interactions represents a formidable task, yet to be accomplished satisfactorily. The realization of experimental simulators [1] therefore constitutes a unique tool for the understanding of fundamental questions in quantum dynamics. Intense theoretical and experimental activities have focused on the out-of-equilibrium dynamics after a sudden change of one of the Hamiltonian parameters (quantum quenches) [2]. Remarkable examples are the observation of a light-cone effect in the spreading of correlations [3, 4], as well as the studies of quantum ergodicity [1, 5–7], where prethermalisation was observed in integrable or nearly integrable systems.

One dimensional systems (1D) are ideal test benches for out-of-equilibrium dynamics because of their intrinsic strong correlations and the possibility to realize integrable models. Moreover, the theoretical understanding of their properties at thermodynamic equilibrium has been consolidated. For the out-of-equilibrium dynamics, however, the lack of systematic *ab initio* treatments calls for experimental quantum simulation. The Lieb-Liniger (LL) model of 1D bosons in continuum, with the Hamilton operator

$$H_{\mathrm{LL}} = \sum_j \frac{p_j^2}{2m} + \sum_{j<k} g_{1\mathrm{D}}\delta(z_j - z_k), \qquad (1)$$

where m is the particle mass, and $g_{1\mathrm{D}}(>0)$ is the coupling constant, is realized experimentally for gases confined in elongated traps, provided the transverse degrees of freedom are frozen out [8]. Various probes have been developed for such gases, permitting not only thermometry methods [9–14] but also the study of nonequilibrium dynamics. Of special importance is the measurement of the momentum distribution via Bragg spectroscopy [15] or focusing technique [14], as its dynamics is particularly elusive in theory. Among the simplest out-of-equilibrium situation is the breathing mode of a harmonically confined gas, after a quench of the potential. Although explored experimentally [16, 17] and theoretically [18, 19], questions such as the effect of temperature remain open. In this Letter, we report an experimental study of the breathing mode of 1D Bose gases confined in a harmonic

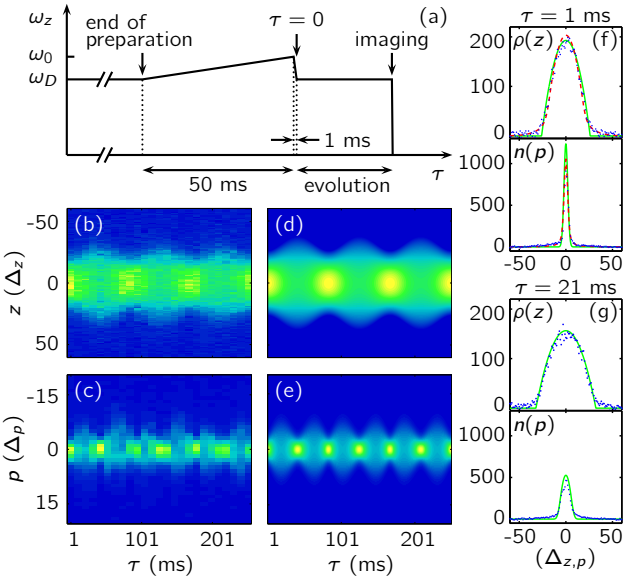

FIG. 1. (Color online) Quench sequence and subsequent density evolution in position and momentum space for a sample in qBEC (data A). (a) Longitudinal trapping frequency ω_z as a function of time τ. (b) $\rho(z,\tau)$, (c) $n(p,\tau)$, experimental data. (d), (e), corresponding plots from *ab initio* scaling calculation. The frequency. (f) and (g) show instantaneous $\rho(z)$, $n(p)$ at $\tau = 1$ and 21 ms. Experimental data (dots) are compared with the scaling solutions (solid lines), and the profiles at thermal equilibrium for the oscillation frequency ω_0 (only in (f), dashed lines). z (p) is in units of pixels Δ_z (Δ_p), with $\Delta_z = 2.7$ μm, and $\Delta_p = 0.14$ $\hbar/\mu$m.

potential, comparing for the first time the evolution in real and momentum space, where very different behaviors are found. We measure how the dynamics evolves through the quasicondensation crossover. Data are compared with theoretical predictions that are derived from an exact short-time expansion and a hydrodynamic approach.

Our experiment uses single 1D samples of ^{87}Rb gas, prepared with an atom-chip setup as detailed in [11]. The final samples typically constitute 800 to 8000 atoms for this experiment. The *in situ* density profile [9] indicates a temperature around 100 nK, corresponding to a central chemical potential $\mu_0 \in [0.04, 0.5] \times k_B T$ [36]. Since the transverse confinement $\omega_\perp = 2\pi \times 2$ kHz, we have $\mu_0 \ll k_B T \simeq \hbar\omega_\perp$, achieving a nearly 1D scenario. The breathing mode is excited by quenching the axial confinement ω_z, see Fig. 1(a) for a sketch. ω_D is determined by monitoring the center-of-mass (dipole) oscillations. We keep the quench strength $\alpha \equiv \omega_0/\omega_D \simeq 1.3$ constant. The resulting cloud is allowed to evolve for a given duration τ before an absorption image is taken, either *in situ* to yield the density profile $\rho(z,\tau)$, or at focus to yield the momentum distribution $n(p,\tau)$. By varying τ, we map out the evolution in real and momentum space, see Fig. 1(b) and (c) for an example (data A) where the samples lie in the quasicondensate (qBEC) regime.

The frequency mismatch revealed by these plots prompts further investigations. We start from the hydrodynamic equations (HDE),

$$\begin{aligned} \partial_\tau \rho + \partial_z(\rho v) &= 0, \\ \partial_\tau v + v\partial_z v &= -\partial_z(\tfrac{1}{2}\omega_D^2 z^2) - \tfrac{1}{m\rho}\partial_z P, \end{aligned} \tag{2}$$

where $\rho = \rho(z,\tau)$ and $v = v(z,\tau)$ are the density and velocity fields, and P is the pressure. For a qBEC, $P = g_{1D}\rho^2/2$, so that the scaling solution $\rho(z,\tau) = \frac{1}{b(\tau)}\rho_0\big(\frac{z}{b(\tau)}\big)$ [21] is valid provided ρ_0 is the steady state inverted parabola, and the scaling factor b obeys $\ddot{b} + \omega_z(\tau)^2 b = \frac{\omega_D^2}{b^2}$. Solutions are periodic with a frequency $\omega_{B_z} \simeq \sqrt{3}\omega_D$ [37]. We show in Fig. 1(d) the calculated real-space evolution for a cloud initially at equilibrium in the trap of frequency ω_0. The scaling solution also implies that the momentum distribution is given by $n(p,\tau) = \left|\frac{b(\tau)}{m\dot{b}(\tau)}\right|\rho_0\Big(\frac{pb(\tau)}{m\dot{b}(\tau)}\Big)$ [21], which is homothetic to the density profile. The divergence of $n(p)$ at times when $\dot{b}(\tau) = 0$ is in reality prevented by thermal fluctuations. On the experiment, however, imaging resolution is the dominant broadening effect. We show in Fig. 1(e) the computed momentum distributions convoluted with an appropriate Gaussian [38]. The results in both real and momentum space agree well with the data. For a more quantitative comparison, we plot $\rho(z,\tau)$ and $n(p,\tau)$ at $\tau = 1$, 21 ms in Fig. 1(f), (g), corresponding to a minimal *in situ* width and a maximal momentum width respectively. Scaling solutions (solid lines) are included in both frames, with $n(p)$ broadened by resolution. Both $\rho(z)$ and $n(p)$ at $\tau = 21$ ms are close to inverted parabolas of the scaling solution, an *ab initio* calculation with no free parameter. We also compare in Fig. 1(f) the measured profiles (dots) at $\tau = 1$ ms with equilibrium theories (dashed lines): $\rho(z)$ is computed using Yang-Yang (YY) equation of state (EoS) [24], while $n(p)$ is computed from quantum Monte Carlo (QMC) methods [14] and broadened by resolution, both under local density approximation [13] with $\omega_z = \omega_0$, and at the temperature obtained from independent calibration without the ω_z ramp. The reasonable agreement provides the grounds for neglecting the effect of the ramp.

The fact that the observed momentum distribution narrows at each *extremum* of the *in situ* width is clear from the scaling solution: the width of $n(p)$ vanishes whenever $\dot{b} = 0$. This is expected at the maximal *in situ* width since the system arrives at the classical turning point. At minimal *in situ* width, on the other hand, the repulsive interactions induce a self-reflection of the cloud. In fact, for small amplitude, we have $b \simeq 1$ and $\dot{b}$ is sinusoidal, so that $n(p)$ is periodic in time with a frequency of $2\omega_{Bz}$ [39], a feature indeed seen in Fig. 1 and Fig. 2 (left column). In higher dimensions, the scaling solutions also predicts a frequency doubling of the breathing modes [40]. What may have prevented its observation is perhaps the fact that early experiments using time-of-flight (TOF) techniques do not measure the true momentum distribution due to the contribution of interaction energy.

We mention in passing that a Tonks gas ($g_{1D} \to +\infty$) [27] also exhibits such a frequency doubling in the oscillatory behavior of the half width at half maximum (HWHM) w_p in momentum space. This can be theoretically obtained from the methods presented in [28]. Similar collective oscillations of strongly interacting 1D Bose gases have been studied in two experiments [5, 17] to our knowledge, neither reporting any second harmonic in the momentum Fourier spectrum. In the former, a different excitation scheme is employed, potentially rendering the frequency doubling inaccessible. In the study of Haller *et al* [17], however, the finite TOF may have prevented the direct measurement of the momentum distribution.

For an ideal Bose gas (IBG), a single-particle description suffices and breathing amounts to a rotation of the phase-space density, so that the widths in real and momentum space oscillate out of phase at the same frequency $\omega_B = 2\omega_D$. Fig. 2 shows a data set close to this regime (data C, right column), where the *in situ* mean-square width $\langle z^2\rangle$ (momentum HWHM w_p) is obtained from Gaussian (Lorentzian) fit. The antiphase is apparent from the plots. Fitting both time evolution with damped sinusoids, we measure identical breathing frequency, $\omega_B/\omega_D = 1.84 \pm 0.04$.

Two questions remain: (i) how ω_{Bz}/ω_D shifts through the crossover, and (ii) in which regime does the momen-

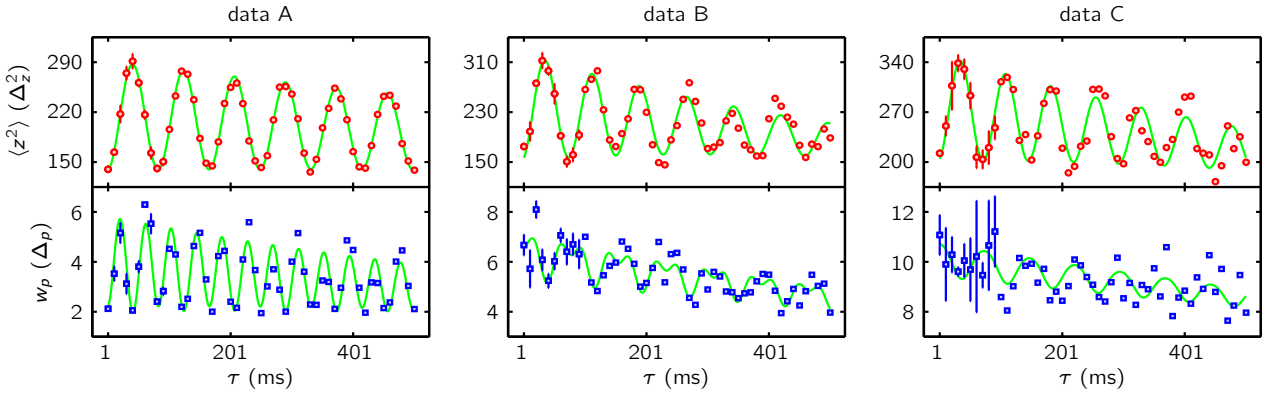

FIG. 2. Time evolution of the *in situ* mean-square width $\langle z^2\rangle$ (top) and the momentum HWHM w_p (bottom) for 3 data sets. The solid lines show the fit: a damped sinusoid in real space (top), and a two-harmonic model according to Eq. (4) in momentum space (bottom). Statistical error of the widths are shown for the first 100 ms.

tum frequency doubling disappear. To address them experimentally, we vary the total atom number in order to traverse the qBEC to IBG crossover. The inset of Fig. 3 shows the region spanned by the data in the (γ, t) phase diagram of the LL model [29], where $\gamma = \frac{mg_{1D}}{\hbar^2\rho}$ is the (local) interaction parameter, and $t = \frac{2\hbar^2 k_B T}{mg_{1D}^2}$ is the reduced temperature. Each sample is characterized by γ_0, evaluated at the peak density. We extract $\langle z^2\rangle$ from fitting $\rho(z)$ with either an inverted parabola for $\gamma_0 < 0.004$ [41] or a Gaussian otherwise, while the w_p is deduced from a Lorentzian fit of $n(p)$.

To answer question (i), we fit $\langle z^2\rangle(\tau)$ with a damped sinusoid to obtain ω_{Bz}. The measured ω_{Bz}/ω_D as a function of γ_0, shown in Fig. 3(a), displays a smooth crossover between the asymptotic theoretical limits $\sqrt{3}$ and 2. Although the sum-rule approach evaluated at $T = 0$ [18] is shown to correctly predict the breathing frequency [17], it is not applicable at finite temperature [42]. Instead, we model the crossover using the HDE Eq. (2). Since long-wavelength density waves in a fluid are adiabatic [43], we use the isentropic pressure curves derived numerically from the YY EoS [24]. The breathing mode frequency measured experimentally does not depend on the breathing amplitude for the explored parameter range. We thus linearize the HDE for small displacement and ω_{Bz} is obtained by solving an eigenvalue problem. Results evaluated at $t = 1100$ are shown as a dashed line in Fig. 3(a). Interestingly, the same results are obtained in an elegant way using an exact short-time expansion. More precisely, we assume the system at $\tau = 0$ is at thermal equilibrium with a Halmiltonian $H = H_{\rm LL} + H_{\rm pot}$, $H_{\rm pot} = m\omega_0^2 \sum_j z_j^2/2$. After the quench $\Delta H = m(\omega_D^2 - \omega_0^2)\sum_j z_j^2/2 = (\frac{1}{\alpha^2} - 1)H_{\rm pot}$, the expansion of the Heisenberg equation of motion gives $\langle \Delta H\rangle(\tau) = \langle \Delta H\rangle_T - \frac{\tau^2}{2}\langle C_2\rangle_T + \frac{\tau^4}{4!}\langle C_4\rangle_T + \ldots$, where $C_2 = [H_f, [H_f, \Delta H]]$ and $C_4 = [H_f, [H_f, [H_f, [H_f, \Delta H]]]]$ are the second and fourth order commutators with $H_f = H + \Delta H$, and the

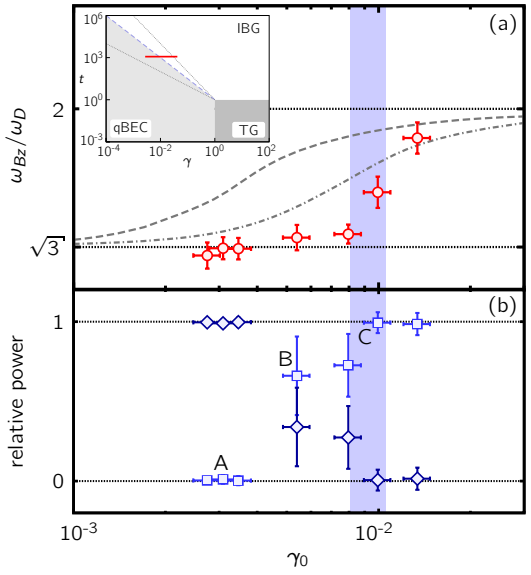

FIG. 3. Breathing mode through the quasicondensation crossover. (a) breathing frequency in units of dipole frequency, as a function of γ_0. Our theory evaluated at $t = 1100$ (dashed line) and $t = 400$ (dash-dotted line) are shown. (b) relative power of the first (square) and doubled (diamond) harmonic of w_p. Data labels (A-C) correspond to those in Fig. 2. The errorbars account for fitting error only. The dotted lines are the asymptotic limits. The shaded region shows the quasicondensation crossover criteria $\gamma_{co} = t^{-2/3}$ (the dashed line in the inset), at $t \simeq 1100$ given by the *in situ* profile up to 20% uncertainly. Inset: the phase diagram of the LL model [29], where all lines represent smooth crossovers. The horizontal line segment gives the region explored by the data [14], whose profile t values are indistinguishable at the scale of the graph.

thermal average $\langle\ \rangle_T$ is taken over the thermal state of H. Suppose the time evolution $\langle \Delta H\rangle(\tau) \propto \langle z^2\rangle(\tau)$ is purely

sinusoidal at the frequency ω_{Bz}, we have

$$\frac{\omega_{Bz}^2}{\omega_D^2} = \frac{\langle C_4\rangle_T}{\langle C_2\rangle_T} = 4 - \frac{1}{2}\frac{\langle H_{\rm int}\rangle_T}{\langle H_{\rm pot}\rangle_T}, \tag{3}$$

where $H_{\rm int} = g_{\rm 1D}\sum_{j<k}\delta(z_j - z_k)$ is the interaction part of the Halmiltonian. The final equality is obtained by explicitly working out $\langle C_2\rangle_T$ and $\langle C_4\rangle_T$, and taking the limit of an infinitesimal quench amplitude $\alpha \to 1$, where the sinusoidal approximation is valid [44]. The qualitative agreement of the theory and data is spoiled by an overestimation of the breathing frequency by both methods. This may indicate that the atomic ensemble is not at thermal equilibrium at the end of the preparation (evaporation). Although the *in situ* profiles calibrated with the YY EoS generally yields about 100 nK, the atom-number fluctuation indicates approximately 35 to 45 nK at the center of the cloud. We thus include in Fig. 3(a) our prediction at $t = 400$ (dash-dotted line). We believe that such a lack of equilibrium is a direct consequence of evaporating into the integrable (1D) regime. Further investigation in this direction is underway.

To address question (ii), we investigate the time evolution of w_p. Since both $\langle z^2\rangle$ and w_p show a periodic behavior at the frequency ω_{Bz}, they can be expanded in a discrete Fourier spectrum. While the fundamental frequency strongly dominates in real space in all regimes, the spectrum of w_p varies across the crossover. We fit w_p with a function

$$y = Ae^{-\frac{\tau}{\tau_1}} + Be^{-\frac{\tau}{\tau_2}}\left[\sqrt{K}\cos(\omega_{Bz}\tau) - \sqrt{1-K}\cos(2\omega_{Bz}\tau)\right], \tag{4}$$

shown in Fig. 2 (bottom, solid line), with A fixed at the average width during the initial cycle and the phase corresponds to a minimal *in situ* width at the start of the oscillations, so that only four free parameters remain. The relative power of the first (squares) and second (diamonds) harmonics, given by K and $1-K$ respectively, are shown in Fig. 3(b) as a function of γ_0. In the qBEC regime, the second harmonic dominates as predicted by the scaling solution, while in the IBG regime, the first harmonic dominates as expected for a noninteracting gas. The relative weight of both harmonics varies gradually through the crossover, indicating a smooth disappearance of the reflection mechanism. This can be seen as the effect the breathing mode has on the thermally excited Bogoliubov modes of high energy, e.g. their frequency and wavefunction would be modulated in time, such that w_p is larger at minimal $\langle z^2\rangle$ than that at maximal $\langle z^2\rangle$, see Fig. 2 (middle column). The periodicity at $2\omega_{Bz}$ is then broken and the first harmonic at ω_{Bz} emerges. Figure 3 shows that the first harmonic starts to gain weight at a value of γ_0 significantly smaller than that where the frequency shift takes place in real space. The possible amplitude dependence of the self-reflection mechanism is not investigated here.

The breathing mode observed has lifetime estimated to be on the order of seconds. This is in stark contrast with situations in 3D where damping of the collective modes occurs, mainly via Landau damping mechanism [34, 35]. The long lifetime of the breathing mode in 1D may be related to the integrability of the underlying LL model.

In conclusion, we have probed the breathing mode in real and momentum space through the quasicondensation crossover. The shift of the frequency between the asymptotic values $\sqrt{3}\omega_D$ and $2\omega_D$ is demonstrated. Our theory models that assume thermal equilibrium before the quench do not agree with the measurement quantitatively, indicating the possibility that the initial state produced by evaporation is not described by Gibbs ensemble. We also report the presence of the second harmonic in the momentum evolution, corresponding to a self-reflection of the cloud, and monitor how it varies through the crossover. No theoretical predictions exist concerning such variation to our knowledge. This illustrates the richness of out-of-equilibrium dynamics and the importance of the momentum-space observation to unveil the underlying physics.

The authors would like to thank A. Minguzzi, S. Stringari, P. Vignolo, M. Zvonarev for stimulating discussions. This work is financially supported by Cnano IdF, the Austro-French FWR-ANR Project I607, and the FP7-Marie Curie IEF grant 327143.

[1] S. Trotzky, Y.-A. Chen, A. Flesch, I. P. McCulloch, U. Schollwöck, J. Eisert, and I. Bloch, Nat. Phys. **8**, 325 (2012).
[2] A. Polkovnikov, K. Sengupta, A. Silva, and M. Vengalattore, Rev. Mod. Phys. **83**, 863 (2011).
[3] T. Langen, R. Geiger, M. Kuhnert, B. Rauer, and J. Schmiedmayer, Nat. Phys. **9**, 640 (2013).
[4] M. Cheneau, P. Barmettler, D. Poletti, M. Endres, P. Schauß, T. Fukuhara, C. Gross, I. Bloch, C. Kollath, and S. Kuhr, Nature **481**, 484 (2012).
[5] T. Kinoshita, T. Wenger, and D. S. Weiss, Nature **440**, 900 (2006).
[6] M. Gring, M. Kuhnert, T. Langen, T. Kitagawa, B. Rauer, M. Schreitl, I. Mazets, D. A. Smith, E. Demler, and J. Schmiedmayer, Science **337**, 1318 (2012).
[7] J. P. Ronzheimer, M. Schreiber, S. Braun, S. S. Hodgman, S. Langer, I. P. McCulloch, F. Heidrich-Meisner, I. Bloch, and U. Schneider, Phys. Rev. Lett. **110**, 205301 (2013).
[8] M. Olshanii, Phys. Rev. Lett. **81**, 938 (1998).
[9] A. H. van Amerongen, J. J. P. van Es, P. Wicke, K. V. Kheruntsyan, and N. J. van Druten, Phys. Rev. Lett. **100**, 090402 (2008).
[10] J. Armijo, T. Jacqmin, K. V. Kheruntsyan, and I. Bouchoule, Phys. Rev. Lett. **105**, 230402 (2010).
[11] T. Jacqmin, J. Armijo, T. Berrada, K. V. Kheruntsyan, and I. Bouchoule, Phys. Rev. Lett. **106**, 230405 (2011).
[12] A. Vogler, R. Labouvie, F. Stubenrauch, G. Barontini, V. Guarrera, and H. Ott, Phys. Rev. A **88**, 031603

(2013).
[13] J. Armijo, T. Jacqmin, K. Kheruntsyan, and I. Bouchoule, Phys. Rev. A **83**, 021605 (2011).
[14] T. Jacqmin, B. Fang, T. Berrada, T. Roscilde, and I. Bouchoule, Phys. Rev. A **86**, 043626 (2012).
[15] N. Fabbri, D. Clément, L. Fallani, C. Fort, and M. Inguscio, Phys. Rev. A **83**, 031604 (2011).
[16] H. Moritz, T. Stöferle, M. Köhl, and T. Esslinger, Phys. Rev. Lett. **91**, 250402 (2003).
[17] E. Haller, M. Gustavsson, M. J. Mark, J. G. Danzl, R. Hart, G. Pupillo, and H.-C. Nägerl, Science **325**, 1224 (2009).
[18] C. Menotti and S. Stringari, Phys. Rev. A **66**, 043610 (2002).
[19] G. E. Astrakharchik, J. Boronat, J. Casulleras, and S. Giorgini, Phys. Rev. Lett. **95**, 190407 (2005).
[36] We remark that other thermometries are possible [13], and seem to indicate a lack of true equilibrium. See the discussions following Eq. 3 for more details.
[21] Y. Castin and R. Dum, Phys. Rev. Lett. **77**, 5315 (1996).
[37] Deviation from $\sqrt{3}\omega_D$ is smaller than 0.3% for $\alpha = 1.3$.
[38] We find a Gaussian point spread function of about 2 pixels in rms width sufficient to account for the broadening.
[24] C. N. Yang and C. P. Yang, J. Math. Phys. **10**, 1115 (1969).
[39] For the oscillation amplitude of the data, a relative weight on the fundamental harmonic at ω_{B_z} as low as 0.01 is predicted.
[40] Both the compression mode and the surface mode for an axially symmetric trap.
[27] M. Girardeau, J. Math. Phys. **1**, 516 (1960).
[28] A. Minguzzi and D. M. Gangardt, Phys. Rev. Lett. **94**, 240404 (2005).
[29] K. V. Kheruntsyan, D. M. Gangardt, P. D. Drummond, and G. V. Shlyapnikov, Phys. Rev. A **71**, 053615 (2005).
[41] The division is justified by the increasingly significant wings for greater values of γ_0.
[42] It predicts $\omega_{Bz} = \sqrt{2}\omega_D$ in the classical limit when one expects $\omega_{Bz} = 2\omega_D$.
[43] No superfluid density is defined in 1D and the two-fluid model that predicts a second sound in higher dimensions do not apply.
[44] Eq. (3) could be used for a quench of finite amplitude ($\alpha \neq 1$) *a priori*. However, in the qBEC regime, a comparison with the scaling solution indicates that the sinusoidal approximation breaks down at finite α.
[34] D. S. Jin, M. R. Matthews, J. R. Ensher, C. E. Wieman, and E. A. Cornell, Phys. Rev. Lett. **78**, 764 (1997).
[35] P. O. Fedichev, G. V. Shlyapnikov, and J. T. M. Walraven, Phys. Rev. Lett. **80**, 2269 (1998).
[36] Note1, we remark that other thermometries are possible [13], and seem to indicate a lack of true equilibrium. See the discussions following Eq. 3 for more details.
[37] Note2, deviation from $\sqrt{3}\omega_D$ is smaller than 0.3% for $\alpha = 1.3$.
[38] Note3, we find a Gaussian point spread function of about 2 pixels in rms width sufficient to account for the broadening.
[39] Note4, for the oscillation amplitude of the data, a relative weight on the fundamental harmonic at ω_{B_z} as low as 0.01 is predicted.
[40] Note5, both the compression mode and the surface mode for an axially symmetric trap.
[41] Note6, the division is justified by the increasingly significant wings for greater values of γ_0.
[42] Note7, it predicts $\omega_{Bz} = \sqrt{2}\omega_D$ in the classical limit when one expects $\omega_{Bz} = 2\omega_D$.
[43] Note8, no superfluid density is defined in 1D and the two-fluid model that predicts a second sound in higher dimensions do not apply.
[44] Note9, eq. (3) could be used for a quench of finite amplitude ($\alpha \neq 1$) *a priori*. However, in the qBEC regime, a comparison with the scaling solution indicates that the sinusoidal approximation breaks down at finite α.